

Article

Mechanochemical Catalytic Transfer Hydrogenation of Aromatic Nitro Derivatives

Tomislav Portada , Davor Margetić  and Vjekoslav Štrukil * 

Division of Organic Chemistry and Biochemistry, Ruđer Bošković Institute, Bijenička cesta 54, 10000 Zagreb, Croatia; Tomislav.Portada@irb.hr (T.P.); Davor.Margetic@irb.hr (D.M.)

* Correspondence: vstrukil@irb.hr; Tel.: +385-1-468-0197

Received: 15 November 2018; Accepted: 29 November 2018; Published: 30 November 2018



Abstract: Mechanochemical ball milling catalytic transfer hydrogenation (CTH) of aromatic nitro compounds using readily available and cheap ammonium formate as the hydrogen source is demonstrated as a simple, facile and clean approach for the synthesis of substituted anilines and selected pharmaceutically relevant compounds. The scope of mechanochemical CTH is broad, as the reduction conditions tolerate various functionalities, for example nitro, amino, hydroxy, carbonyl, amide, urea, amino acid and heterocyclic. The presented methodology was also successfully integrated with other types of chemical reactions previously carried out mechanochemically, such as amide bond formation by coupling amines with acyl chlorides or anhydrides and click-type coupling reactions between amines and iso(thio)cyanates. In this way, we showed that active pharmaceutical ingredients Procainamide and Paracetamol could be synthesized from the respective nitro-precursors on milligram and gram scale in excellent isolated yields.

Keywords: mechanochemistry; catalytic transfer hydrogenation; aromatic nitro derivatives; ammonium formate; aging; ball milling; synthesis

1. Introduction

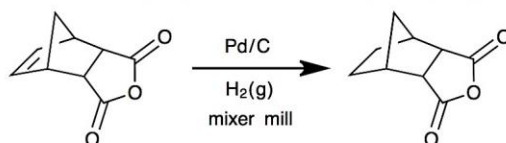
Catalytic hydrogenation is one of the most significant functional group transformation reactions in organic synthesis and numerous procedures and reagents have been developed for that purpose [1,2]. As such, the hydrogenation reaction plays one of the key roles in many industrially important processes, for example hydrogenation of carbon monoxide to methanol or in food industry for the conversion of unsaturated vegetable oils into saturated triglycerides [3]. From a variety of available protocols, we have selected to use of formic acid salts as the source of hydrogen as a particularly appealing methodology [4–6]. In the presence of a catalytic amount of palladium on carbon, ammonium formate undergoes decomposition to carbon dioxide, ammonia and hydrogen [7]. This type of hydrogenation reaction is typically performed in a solvent by stirring a heterogeneous mixture until the reaction is complete. Following the emergence of new greener methods for chemical synthesis, ammonium formate promoted hydrogenation has been attempted under microwave irradiation [8,9] and in ionic liquids [10]. Mechanochemistry by ball milling has attracted much attention in the chemistry community as a promising methodology that meets many of the green chemistry criteria [11–15]. Its effectiveness is reflected in often quantitative reaction yields and short reaction times, high product purity, low energy consumption and cost. Simple sample preparation that avoids bulk solvent and bench-top operation mode make it suitable for research and educational laboratories [16], whereas the application of twin extrusion allows large scale solid-state synthesis of compounds [17–19]. Novel methodological concepts, such as resonant acoustic mixing, enable an efficient solid-state synthesis of pharmaceutical cocrystals [20] while technical solutions like multiposition jars/adapters and ball milling compatible LED reactors and glass jars, assist in

broadening the utility of mechanochemistry in high-throughput parallel synthesis [21] and solid-state visible light photocatalysis [22].

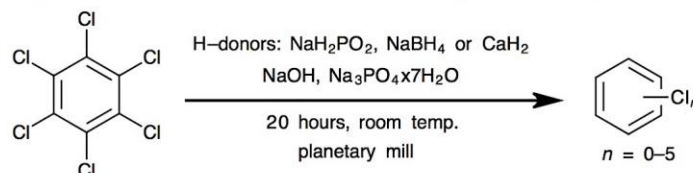
Therefore, one can envisage that hydrogenation reaction might also be transferred into the arena of mechanochemically-assisted organic synthesis [23–27]. Significant progress has been made over the last several years in this respect, with mechanochemistry securing its place in organic chemistry areas like organocatalysis [28–30] and metal-catalysis [31], C–H functionalization [32,33], multicomponent reactions [34] and so forth. Considering the expansion of literature on utilising solid-state milling as a synthetic tool, the mechanochemical hydrogenation still remains one of the underexplored areas with only a few papers published (Scheme 1).

Previous work:

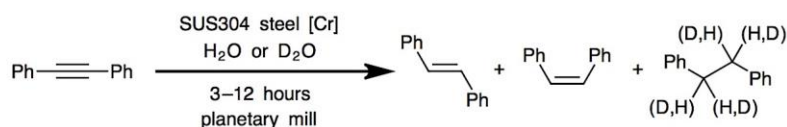
- Mechanochemical gas-solid hydrogenation in H₂ atmosphere (Kaupp, unpublished)



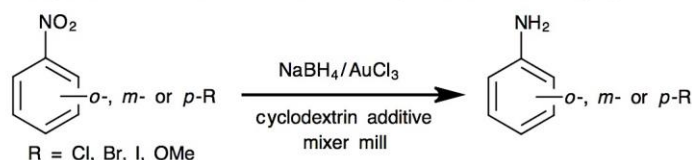
- Mechanochemical hydrodechlorination of chloroaromatic hydrocarbons (Pri-Bar & James, 2007)



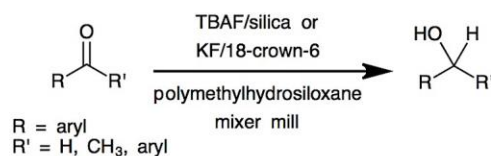
- Stainless-steel ball-milling hydro/deutero-generation (Sawama, 2015)



- AuNP-catalyzed reduction of nitrobenzenes with cyclodextrin additives (Hapiot, 2016)

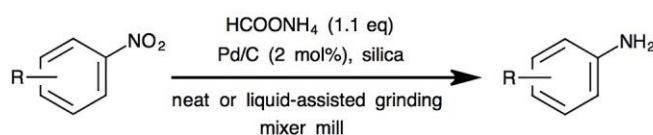


- Mechanochemical transfer hydrogenation of carbonyls (Moores & Li, 2017)



This work:

- Mechanochemical catalytic transfer hydrogenation of nitroarenes using ammonium formate



R = NH₂, NO₂, OH, COOH, CN, NHCOR', halogen, urea, ketone, amino acid

Scheme 1. Selected recent examples of hydrogenation reactions under mechanochemical conditions.

For example, Delogu reported hydrogenation of carbon monoxide over solid $(\text{Co}_{50}\text{Fe}_{50})_{0.2}(\text{TiO}_2)_{99.8}$ and $\text{Ni}_{40}(\text{ZrO}_2)_{60}$ catalysts under ball milling conditions [35], while Mack et al. developed a mechanochemical approach for the hydride reduction of esters to alcohols using $\text{NaBH}_4/\text{LiCl}$ system [36]. An example of catalytic hydrogenation reaction using Pd/C as the catalyst under a pressure of hydrogen gas (unpublished results) was provided in a review by Kaupp [37], who described the gas-solid synthesis of norbornane-*endo*-2,3-dicarboxylic anhydride from the norbornene derivative in 200 g batches. The product was easily sublimed off from the catalyst but milling was not applicable if volatile liquids had to be constantly pumped off or if the products had become liquid or sticky. A few literature sources report on the mechanochemical reductive dehalogenation [38–40], for example catalytic hydrodechlorination of aromatic chlorinated compounds such as hexachlorobenzene by using calcium hydride, sodium hypophosphite or borohydride as the hydride donors in a ball mill [41]. Sawama reported on an interesting example of hydro- and deuterogenation of unsaturated substrates by H_2O or D_2O as H_2 or D_2 sources in a planetary ball mill. Chromium and nickel, as structural components of SUS304 stainless steel jars and balls used in experiments, reduce $\text{H}_2\text{O}/\text{D}_2\text{O}$ generating H_2/D_2 in situ under rather harsh milling conditions [42,43]. In their latest report, in-situ generation of hydrogen gas from alkanes or even diethyl ether was demonstrated [44]. Hapiot et al. described gold nanoparticles-catalysed (AuNPs) reduction of several *o*-, *m*- and *p*-halogenated nitrobenzene derivatives by ball milling. With sodium borohydride as the reducing agent, cyclodextrin-stabilised AuNPs were employed as catalysts to achieve nitro-group reduction [45]. Most recently, Moores and Li employed milling for the catalytic transfer hydrogenation (CTH) of ketones and aldehydes to alcohols using polymethylhydrosiloxane with either tetrabutylammonium fluoride/silica or potassium fluoride/18-crown-6 mixtures as additives [46]. The authors demonstrated a successful reduction of the carbonyl group in the presence of potentially reactive functionalities such as alkenes or alkynes, carboxylic, cyano and nitro groups.

The reduction of aromatic nitro-group is a well-documented organic transformation [47–54]. Traditionally, the reaction is carried out in a suitable solvent under an atmosphere of hydrogen in the presence of a catalyst. Hydrogen gas can also be generated by the action of an acid (HCl or acetic acid) on metals such as zinc, iron or indium where electron transfer produces reduced radical species or indirectly from hydrogen transfer reagents (donors), for example formate salts or hydrazine. Except for the AuNP-catalysed reduction of halogenated nitrobenzenes using NaBH_4 [45], it seems that mechanochemical approach has otherwise not been employed for the conversion of nitroaromatics to substituted anilines.

Here, we opted for easy-to-handle crystalline ammonium formate as a cheap, water soluble and low hazard hydrogen source which, in combination with Pd-C catalyst and silica as the only additive, allows for an environmentally-friendly mechanochemical catalytic transfer hydrogenation (CTH) of aromatic compounds containing the nitro functionality (Scheme 1). This method also avoids working with pressurized hydrogen gas which requires a special experimental setup and enables simple and easy-to-implement procedure in research laboratories but also in organic chemistry education as a model mechanochemical reduction reaction. Still, precautions are advised since aromatic nitro derivatives are toxic and potentially explosive.

In this paper, we demonstrate how simple milling of the reactant mixture in a ball mill provides an environment for efficient synthesis of a series of aromatic amines by CTH of nitro derivatives, particularly targeting biologically active compounds such as procainamide and paracetamol. Selected reactions have also been carried out on 1.0 g scale, whose efficiency matched the milligram scale ones.

2. Results and Discussion

Initially, all reactions were carried out by grinding a mixture of a nitroarene, ammonium formate and palladium on carbon (10 wt%) under solvent-free or neat grinding (NG) conditions. While CTH reactions in solution typically require 1.5–2.0 equivalents of ammonium formate as hydrogen source and extensive solvent extraction purification [55,56], solid-state milling approach allowed the loading

to be decreased to 10 mol% excess with simple filtration-based work-up. However, a practical problem of diminished isolated yields was encountered in all cases due to inefficient mixing and recovery of the crude product caused by its sticky nature. For that reason, we employed silica as an inert solid support, which improved the appearance of the crude mixture to fine powder, enabling quantitative recovery of the material from the grinding jar. Due to build-up of pressure during the reaction, the jars were carefully opened in a well ventilated fume hood to allow safe release of gaseous by-products (CO_2 and strong odour of NH_3).

The advantage of performing the solid state ammonium formate promoted hydrogenation reaction is revealed in Figure 1b. The rate of 3-nitrobenzonitrile (**1a**) reduction as a model reaction (Figure 1a) in methanol (solution reaction) at room temperature using the same molar quantities of reactants as in milling reaction (1.1 eq of formate, 2 mol% of Pd/C (10 wt%)) shows partial conversion to product **2a** (ca. 70% after 90 min) monitored by HPLC. In the case of mechanochemical synthesis, the LAG reaction reaches quantitative conversion in 60 min [57]. We note that 3-nitrobenzonitrile reduction under neat grinding conditions is much less efficient in comparison with LAG reaction, reaching only ca. 55% conversion after 90 min. As previously demonstrated for mechanochemical amination of thiocarbamoyl benzotriazoles, the physico-chemical interaction of in situ formed gases and liquids used in LAG can have a profound effect on the outcome of milling reactions [58].

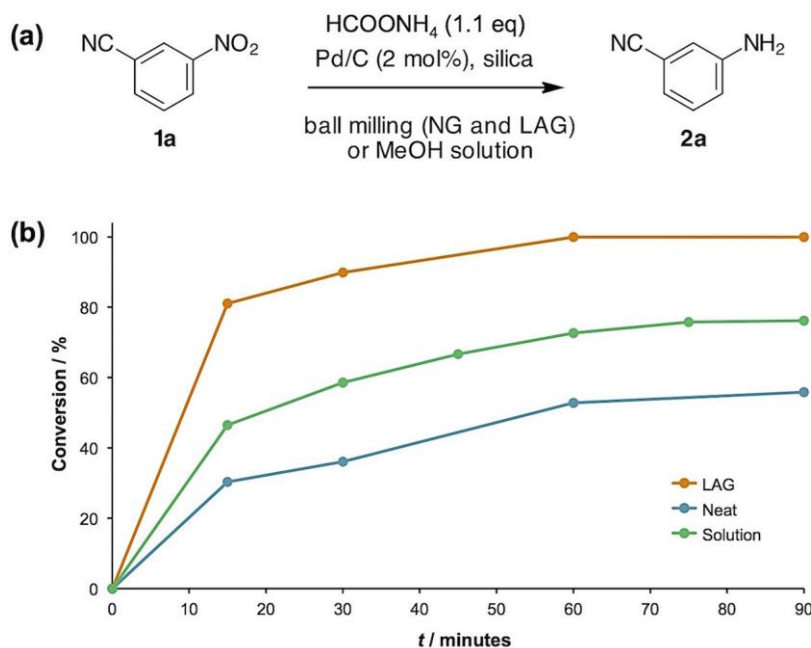


Figure 1. (a) Mechanochemical CTH model reaction; (b) Conversion of 3-nitro-benzonitrile during CTH determined by HPLC analysis. *Reaction conditions:* 3-nitrobenzonitrile (1.0 mmol), ammonium formate (3.3 mmol, 1.1 equivalent), 10 wt% Pd/C (21 mg, 2 mol%). In milling experiments, a 10 mL grinding jar containing one 12 mm stainless steel ball was charged with silica (175 mg) as an additive and 137 μL of methanol (LAG). The solution reaction was performed in methanol (10 mL) with stirring (1000 rpm) at 22 °C.

Surprisingly, we note that the model reaction did not take place under aging conditions in open air, that is, without an extensive mechanical agitation. For example, when the reaction mixture was gently homogenized by brief manual grinding (ca. 2–3 min) in a mortar and left open at room temperature (25 °C) for 3 days, TLC, FTIR-ATR and ^1H NMR analyses indicated complete absence of 3-cyanoaniline (**2a**) (Figure 2a–d). IR analysis also revealed quantitative decomposition of ammonium formate where only the characteristic absorption bands of the reactant **1a** (3079, 2236, 1617, 1529, 1353, 734 and 668 cm^{-1}) and silica (1068 cm^{-1}) were identified. Quantitative decomposition of HCOONH_4 rapidly took place (2 h) in air when the nitro-substrate was left out. On the other hand,

milling Pd/C-silica-HCOONH₄ mixture without **1a** for 60 min resulted in partial decomposition of ammonium formate under neat or LAG conditions (ca. 20% conversion, Figure 2g) [59]. Comparison of IR spectra showed complete disappearance of the characteristic HCOONH₄ absorption bands (2794, 1704, 1585, 1342 and 773 cm⁻¹) on aging these mixtures overnight in air (Figure 2h), which is consistent with the observations in attempted aging of the model reaction. We conclude from these experiments that in open air ammonium formate undergoes Pd-catalysed decomposition to hydrogen (H₂), carbon dioxide (CO₂) and ammonia (NH₃) gases, without affecting the reduction of the nitro substrate when present.

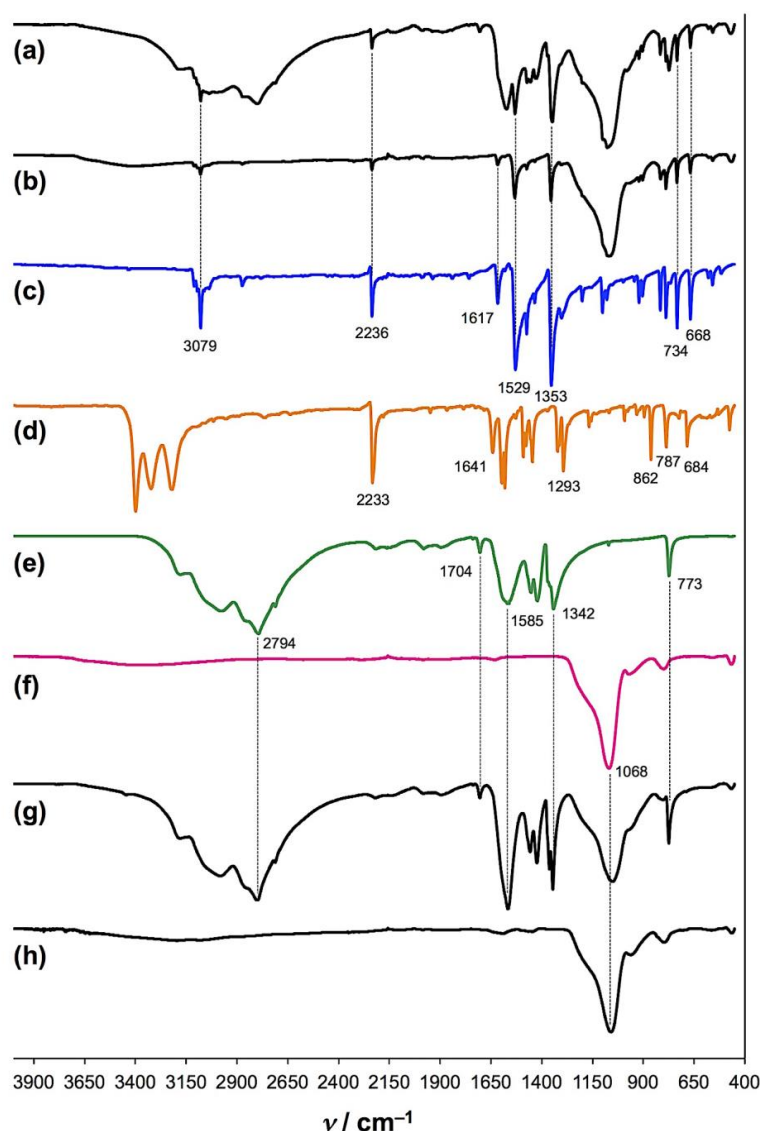


Figure 2. FTIR-ATR monitoring of aging reactions in open air. Reaction mixture after (a) gentle manual grinding for 2–3 min; (b) aging for 3 days; (c) 3-nitrobenzonitrile (**1a**); (d) 3-cyanoaniline (**2a**); (e) ammonium formate; (f) silica; (g) LAG for 60 min without substrate **1a**; (h) LAG-mixture under (g) after aging for 2 h in air.

Next, the **1a**-Pd/C-silica-HCOONH₄ mixture (0.5 mmol scale) was left undisturbed in a sealed 10 mL milling jar for 3 days. ¹H NMR analysis showed 59% yield of aniline **2a**, suggesting that the reaction could take place even by aging but in a closed system. To verify this hypothesis, an experiment was designed where the model reaction mixture (0.5 mmol scale) underwent aging in glass vials of different volume, that is, 2, 5, 10, 20 and 50 mL. The 50 mL vial simulated an “open system”

whereas smaller vials represented “closed systems” (Figure S2, ESI). In this way, by decreasing the reactor volume from 50 to 2 mL, the effect of internal pressure increase was achieved. After 3 days of aging, ^1H NMR analyses confirmed that the model reaction did not proceed in the largest 50 mL vial. On contrary, the product yield in 20 mL vial averaged at 15% and levelled off at around 60% in 2, 5 and 10 mL vials (Figure 3a). The solid reaction mixtures were then left undisturbed in open air for 24 h and analysed by IR and NMR spectroscopy. As expected, IR spectra showed complete disappearance of ammonia formate absorption bands, initially present upon opening the vials (Figures S4 and S5) while ^1H NMR revealed no or only minor changes in the composition of the reaction mixtures (Figure S3). These results indicate a strong correlation between the product yield and pressure but also provide some insight into the possible reaction mechanism outlined in Figure 3b.

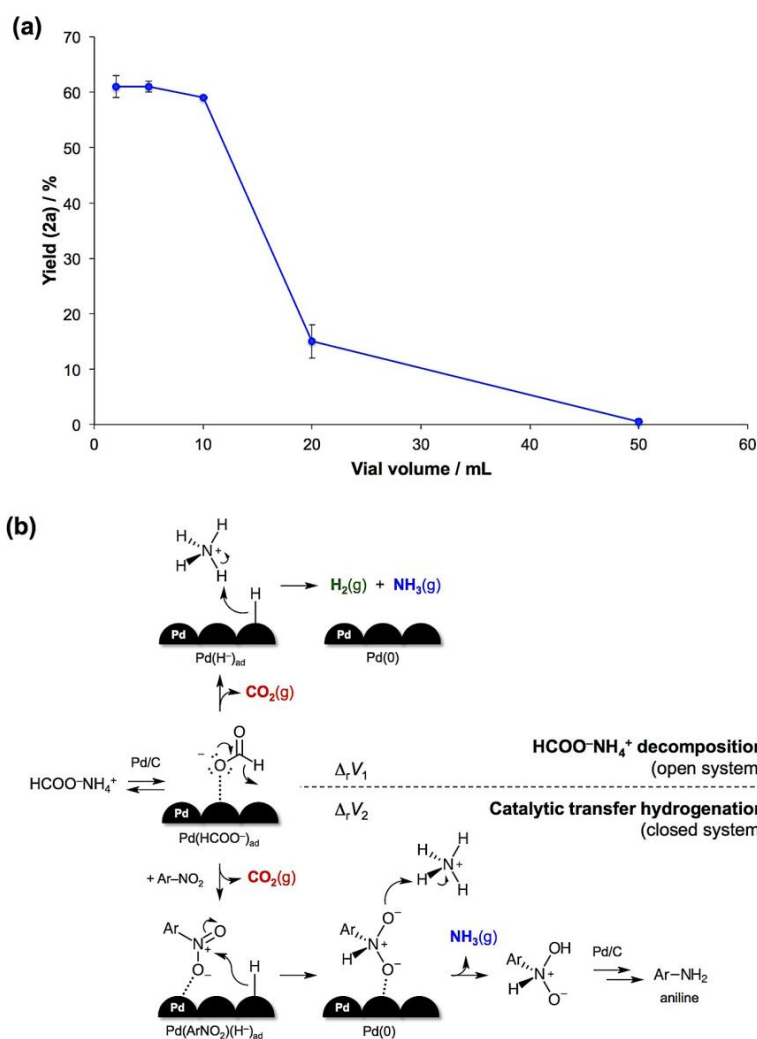


Figure 3. (a) The yield of 3-cyanoaniline (2a) vs. vial volume during aging reactions at room temperature; (b) Proposed reaction mechanism with preferred reaction paths in open and closed systems.

Previous studies postulate the adsorption of formate ion on the surface of Pd-catalyst as the first step ($\text{Pd}(\text{HCOO}^-)_{\text{ad}}$) [60–62]. Upon release of CO_2 molecule and formation of activated Pd-hydride species (labelled as $\text{Pd}(\text{H}^-)_{\text{ad}}$), ammonium cations acting as Brønsted acid protonate these hydride species, generating hydrogen and ammonia gases. Alternatively, substrate molecules compete with NH_4^+ ions for $\text{Pd}(\text{H}^-)_{\text{ad}}$ sites and following the hydride transfer to NO_2 -group, the resulting intermediate is protonated by NH_4^+ with the release of NH_3 molecule. These species then re-enter the catalytic cycle and eventually afford the aniline product (which explains the required substrate:donor =

1:3 stoichiometry). While Pd-catalysed HCOONH_4 decomposition generates 3 equivalents of gaseous products (H_2 , CO_2 and NH_3) per 1 equivalent of the salt, during CTH reaction 2 equivalents are released (CO_2 and NH_3). The respective reaction volume changes are denoted as $\Delta_r V_1$ and $\Delta_r V_2$, whereas $\Delta_r V_1 > \Delta_r V_2$ [63]. This implies that the former reaction ($\Delta_r V_1$) is more susceptible to pressure changes than the latter one ($\Delta_r V_2$). In particular, in accordance with Le Chatelier's principle an increase in the internal pressure should suppress the reaction with larger $\Delta_r V$, in our case ammonium formate decomposition. However, this reaction pathway is preferred in an open system (large reactor volumes or completely exposed to air) where gases freely escape the reaction mixture and due to irreversibility of this process, the reduction of NO_2 -group does not occur. In a closed system, the preferred reaction path would be CTH as it is less sensitive to higher internal pressure. The competition between these two possible reaction channels is best reflected in higher conversion of **1a** and increased yield of **2a** on reducing the reactor volume (Figure 3a). When the **1a**-Pd/C-silica- HCOONH_4 mixture (0.5 mmol scale) was briefly ball milled in a 10 mL jar for only 2 min, prior to aging for 3 days at room temperature, the yield of **2a** reached 88%. This also illustrates the importance of ball milling for the efficiency of CTH since the introduction of mechanical agitation into the aging system alleviates the 60% yield plateau and facilitates effective mixing, mass transfer and fresh surface exposure, thus allowing for a quantitative synthesis of **2a** and a number of other aromatic derivatives in 90 min (Table 1). Finally, the dual reactivity was exploited in the isolation procedure where a slight excess of HCOONH_4 is efficiently removed from the crude reaction mixture by allowing it to stand in air overnight and decompose to gaseous by-products.

In the studied system, an important consideration is the effect of milling on the particle size and their morphology. Samples of commercial and milled Pd/C catalyst, as well as the catalyst milled in the presence of silica were analysed by scanning electron microscopy (SEM) as shown in Figure 4. Energy-dispersive X-ray spectroscopy (EDS) analysis indicates that palladium is organized into aggregates of different sizes adsorbed on the surface of carbon particles (Figures S6 and S8). On milling for 60 min, their size and morphology drastically change and the sample becomes more homogeneous with palladium distribution more uniform as suggested by EDS analysis (Figures S7 and S9). Similar effect is observed in Pd/C milled with silica where the average particle size achieved after 60 min of LAG (methanol, 12 mm ball size, 30 Hz) is estimated at ca. 0.1–1.0 μm . Analysis of the catalyst milled with silica under solvent-free conditions reveals similar average particle size range, suggesting that LAG has no influence on particle size in this system.

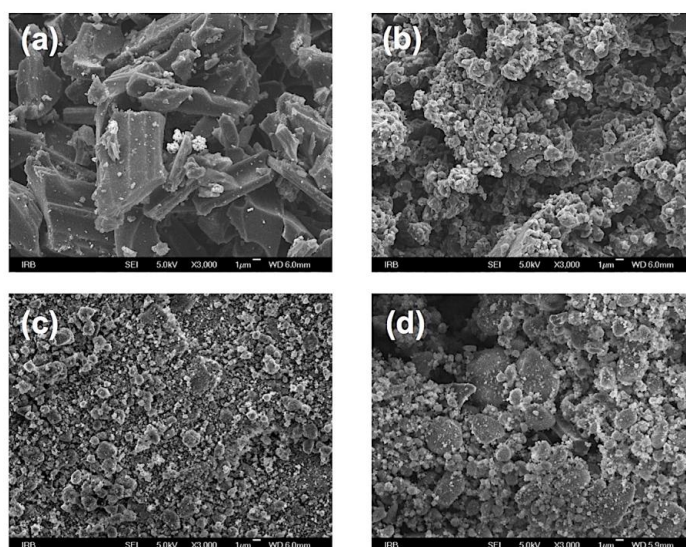
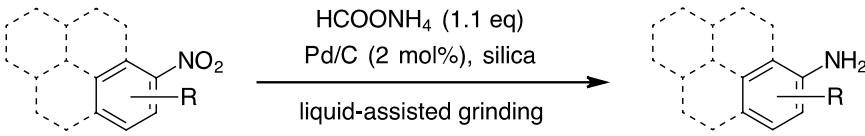
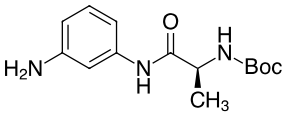
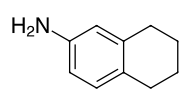
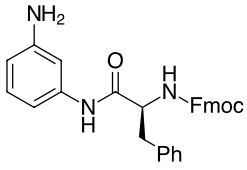
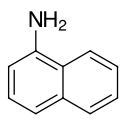
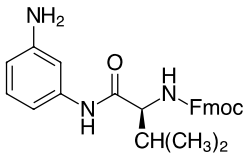
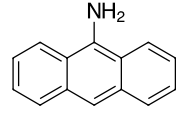
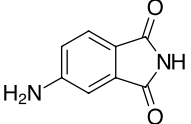
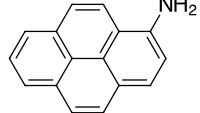


Figure 4. SEM images (3000 \times) of (a) commercial and (b) milled samples of 10 wt% Pd/C catalyst; (c) The catalyst milled with silica under LAG conditions for 60 min and (d) post-workup sample after CTH of 3-nitrobenzonitrile.

Table 1. The scope of mechanochemical catalytic transfer hydrogenation ¹.

1b-z		2b-z	
Product	Yield ²	Product	Yield
	<i>o</i> -2b, 99% (99%) <i>m</i> -2b, 98% (96%) <i>p</i> -2b, 95% (96%)		2n-S, n.r. (X=S) 2n-O, 96% (X=O)
	<i>o</i> -2c, 99% <i>m</i> -2c, 94% <i>p</i> -2c, 99%		2o, 95% ³
	<i>o</i> -2d, 98% <i>m</i> -2d, 99% <i>p</i> -2d, 97%		<i>p</i> -2p, 17%
	2e, 99%		<i>o</i> -2p, 42%
	2f, 99%		2q, 37%
	2g, 94%		<i>m</i> -2r, 99% (R=Ph) <i>p</i> -2r, 99% (R=Ph)
	2h, 93%		2s, 95%
	2i, 99%		2t, 95% (R=H) 2u, 84% (R=Me)
	2j, 99%		2v, 90%

Table 1. Cont.

			
1b-z		2b-z	
Product	Yield ²	Product	Yield
	2k, 99%		2w, 40% (97%) ³
	2l-Phe, 93% ³		2x, 18% (37%)
	2l-Val, 90% ³		2y, traces
	2m, 97%		2z, n.r.

¹ Reaction conditions: 1.0 mmol substrate, 3.3 mmol HCOONH₄, 2 mol% of Pd/C and 175 mg of silica were ground in a 10 mL jar using one 12 mm stainless steel ball at 30 Hz for 90 min. Methanol was used for LAG ($\eta = 0.25 \mu\text{L mg}^{-1}$). ² For 2b isomers, yields in the parentheses refer to CTH of the respective dinitrobenzenes on 0.75 mmol scale. ³ For compounds 2l-Phe, 2l-Val, 2o and 2w, 2.2 eq of HCOONH₄ and 5 mol% of Pd/C were required, while for 2j, p-2p and o-2p, blue colour indicates the position of the reduced nitro group. Other details can be found in the Supplementary Materials.

Following the initial studies on the reduction of 3-nitrobenzotrile (1a) to 3-cyanoaniline (2a), we focused our efforts on investigating the scope of mechanochemical CTH reaction (Table 1). Simple nitroaromatic derivatives such as *o*-, *m*- and *p*-nitroanilines and phenols gave the respective phenylenediamines (*o*-, *m*- and *p*-2b) and aminophenols (*o*-, *m*- and *p*-2c) in almost quantitative yields. 1,2-, 1,3- and 1,4-dinitrobenzenes also smoothly underwent the reduction and led to excellent isolated yields of phenylenediamines (*o*-, *m*- and *p*-2b). The same results were obtained with *o*-, *m*- and *p*-nitrobenzoic acids, 3,5-dinitrobenzoic acid and 2-nitrotterephthalic acid as the carboxylic group containing substrates, which all efficiently gave aminobenzoic acids 2d–f. Next, we wanted to investigate the compatibility of our mechanochemical approach with different protecting groups, for example acetyl, ethyl carbamoyl, *tert*-butoxycarbonyl (Boc) and 9-fluorenylmethyloxycarbonyl (Fmoc). Gratifyingly, in all cases the protecting group survived the reduction conditions and afforded substituted anilines 2g–j in high yields. In the case of amino acid derivatives, the Boc-protection in alanine compound 2k, as well as Fmoc-protection present in phenylalanine compound 2l-Phe and valine product 2l-Val did not interfere with the reduction of the nitro group which proceeded in a straightforward and clean fashion. This result is in contrast to the reported Fmoc-deprotection of amino acids which was accomplished under relatively mild conditions by hydrogenation (1 atm, balloon) in methanol solution using 10 wt% of Pd/C catalyst [64]. 4-Nitrophthalimide (1m), as a model compound containing the imide functionality, was also quantitatively converted to 4-amino-phthalimide (2m).

Expectedly, *N*-(3-nitrophenyl)-*N'*-phenylthiourea (1n-S) did not react as it is known from literature that sulphur is not compatible with this type of hydrogenation reaction due to catalyst poisoning [65,66].

On the other hand, the presence of an oxygen atom in the analogous *N*-(3-nitrophenyl)-*N'*-phenylurea (**1n-O**) did not affect the catalyst activity and led to an excellent 96% isolated yield of aminophenylurea **2n-O** in 90 min. 3-Nitroacetophenone **1o** only partially reacted under standard 1.0 mmol scale conditions. This reduction resulted in 11% conversion to the product **2o** in 90 min but increasing the ball-to-reactant ratio [67] from 10.6 to 21.1 by lowering the scale to 0.5 mmol, as well as increasing the HCOONH₄ and Pd/C loadings to 2.2 eq and 5 mol%, proved beneficial providing 3-aminoacetophenone (**2o**) in 95% isolated yield after 6 h milling.

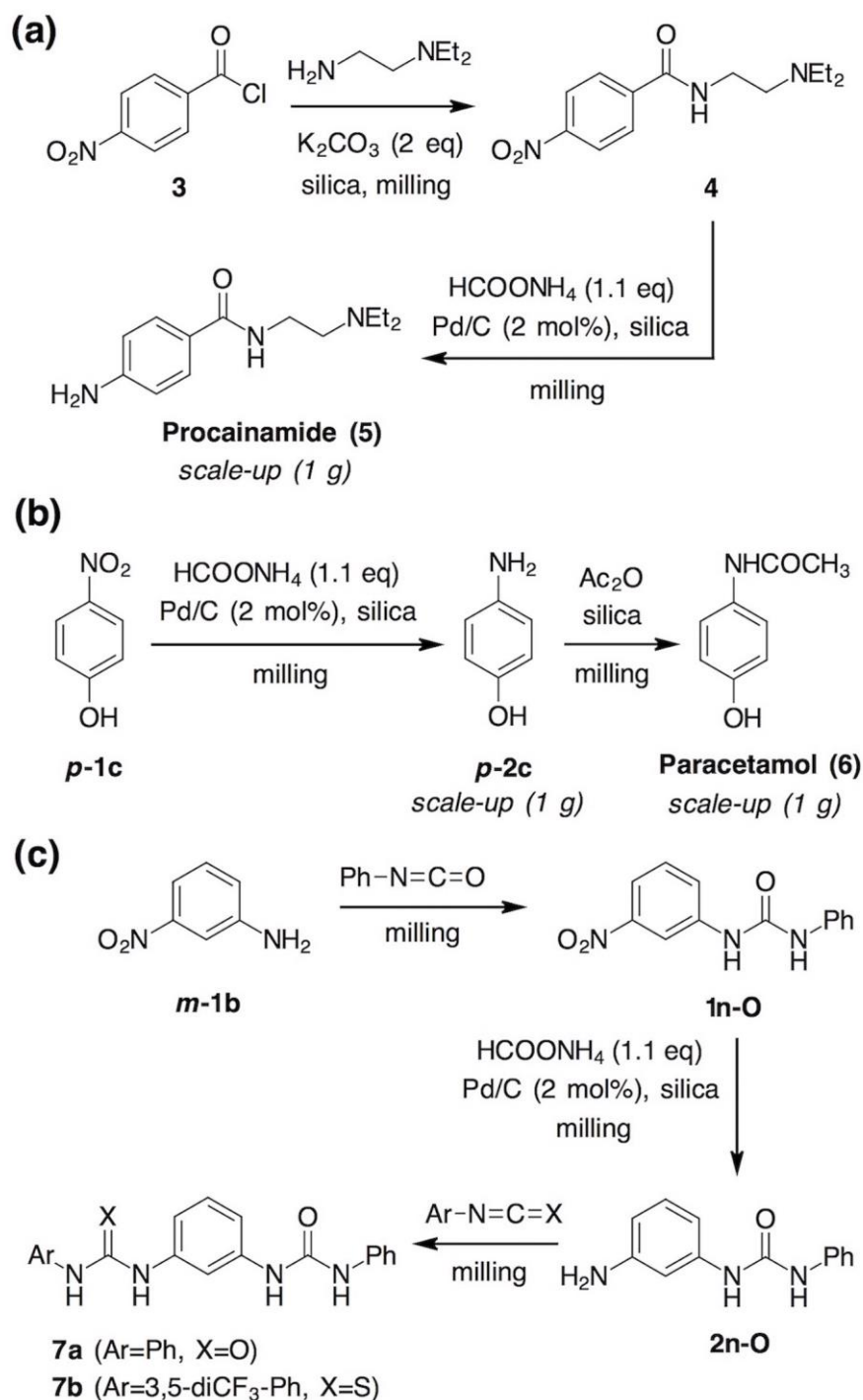
In the case of halogen-substituted nitroarenes, for example 2-chloro-4-nitroaniline (**p-1p**) and 4-chloro-2-nitroaniline (**o-1p**), CTH with 1.1 eq of ammonium formate gave a mixture of the hydrogenation and dehalogenation products after 90 min of LAG, as established by GC analysis. Following chromatographic separation, 2-chloro-1,4-phenylenediamine (**p-2p**) (17%) and 4-chloro-1,2-phenylenediamine (**o-2p**) (42%) were isolated. Interestingly, MS analysis of polar fractions (MeOH as eluent) from the reduction of 4-chloro-2-nitroaniline (**o-1p**) indicated the presence of compounds with *m/z* values 212 and 246, which correspond to 2,2'-diaminoazobenzene and 2,2'-diamino-4-chloroazobenzene, respectively (Figure S10, ESI). According to the generally accepted mechanism of NO₂ to NH₂ reduction [51,53], azobenzene species have been proposed as reactive intermediates, implying that in our case the CTH reaction was not complete despite almost quantitative conversion of the starting nitro derivatives **p-1p** and **o-1p**, as shown by GC analyses (Figures S11–S13). This is the result of HCOONH₄ being consumed for the cleavage of carbon-chlorine bond, which disrupts the stoichiometry required for a quantitative reduction to the amino product. Unfortunately, increasing the amount of the hydrogen donor to 2.2 eq (6.6 mmol) or catalyst loading to 5.0 mol% again led to dehalogenation as the primary reaction pathway. Similarly, a selective NO₂-reduction in the presence of *O*-benzyl protecting group in compound **1q** failed with only 37% yield of the desired amino-derivative **2q** after chromatographic purification. Here, the cleavage of *O*-Bn bond competes with the reduction of NO₂ group leading to a mixture of unreacted **1q**, **2q**, **p-1c** and **p-2c** (4-nitro- and 4-aminophenol).

As examples of α,β -unsaturated carbonyl compounds, *m*- and *p*-nitrochalcones **m-1r** and **p-1r** were subjected to mechanochemical reduction. While the respective aminochalcones **m-2r** and **p-2r** were isolated in quantitative yields, we did not observe reduction of the carbonyl groups in these reactions, which makes the proposed synthetic protocol complementary to the recently published CTH of aldehydes and ketones [46]. The quantitative conversion was also observed for 4-nitrotoluene (**1s**) which gave 95% of *p*-toluidine (**2s**) after isolation. CTH of the corresponding nitro substrates **1t**, **1u** and **1v** efficiently afforded 5-aminoquinoline (**2t**), 5-amino-4-methylquinoline (**2u**) and 8-aminoquinoline (**2v**) as representatives of pyridine-fused nitroaromatics.

The most challenging substrates were found to be polyaromatic nitro derivatives, for example 1-nitronaphthalene (**1x**), 9-nitroanthracene (**1y**) and 1-nitropyrene (**1z**) where GC analysis showed only traces of 9-aminoanthracene after 6 h of milling and no reaction with the pyrene compound. Naphthalene derivative **1x** displayed some reactivity based on NMR analysis of the crude reaction mixture. Under standard conditions (1.0 mmol, 90 min), 18% of 1-aminonaphthalene (**2x**) was obtained while prolonging the reaction time to 6 h increased the yield to 37% [68]. Interestingly, 6-nitrotetralin (**1w**) was more reactive and afforded 40% of 6-aminotetralin (**2w**) after 90 min. Still, quantitative conversion to **2w** required 2.2 eq of HCOONH₄ (6.6 mmol), 5 mol% of Pd/C and 3 h of milling.

Finally, we wanted to demonstrate the utility of mechanochemical CTH reaction in the multi-step milling syntheses of two active pharmaceutical ingredients (API) and two structural analogues of urea-type anion sensors. The first example describes a successful two-step preparation of an API procainamide (**5**). Procainamide is classified as a sodium channel blocker used in treatment of cardiac arrhythmia, administered orally or intravenously [69]. Previously, there have been several attempts at utilizing mechanochemistry for the synthesis of biologically active compounds and APIs [70], for example teriflunomide [71], Leu-enkephalin [72], atorvastatin [73] and several sulfonylureas [74].

Here we wish to extend the list of useful marketed drugs amenable to mechanochemical milling synthesis (Scheme 2).



Scheme 2. Two-step mechanochemical synthesis of active pharmaceutical ingredients (a) procainamide (5); (b) paracetamol (6) by coupling mechanochemical nitro-group reduction, amide formation and acetylation; (c) Integration of CTH with amine-iso(thio)cyanate coupling for the mechanochemical three-step synthesis of bis (thio)ureas **7a–b**. For details, see Supplementary Materials.

Excellent conversion of 4-nitrobenzoic acid to 4-aminobenzoic acid (*p*-2d) was further explored in CTH reaction of 4-nitrobenzoyldiethylethylenediamine (**4**) which is a precursor for procainamide on the industrial scale synthesis. A two-step procedure, consisting of amide coupling followed by

catalytic transfer hydrogenation, was employed to prepare **5** by solid state ball milling. The formation of amide **4** in the first step was accomplished through mechanochemical K_2CO_3 -assisted coupling of solid 4-nitrobenzoylchloride (**3**) (1.1 eq) with *N,N*-diethylethylenediamine in the presence of silica as the milling auxiliary [75,76]. Simple extraction with ethyl acetate furnished the pure nitro intermediate **4** in 88% yield. In the next step, **4** was subjected to CTH under LAG conditions using methanol to afford procainamide (**5**) quantitatively in 90 min (Scheme 2a). As in previous examples, the crude reaction mixture was suspended in methanol, followed by filtration and evaporation of the solvent, yielding the target drug **5**. The CTH of nitro-precursor **4** can be scaled-up to 5.0 mmol, affording 1.18 g of procainamide (**5**) in quantitative yield after 6 h of milling.

Furthermore, 4-aminophenol (**p-2c**) obtained by mechanochemical hydrogenation of *p*-nitrophenol (**p-1c**) was successfully utilized for the rapid and quantitative solvent-free synthesis of paracetamol (**6**), a widely used analgesic and antipyretic active pharmaceutical ingredient (API) (Scheme 2b). Acetylation of the amino group was in this case accomplished by milling an equimolar mixture of **p-2c** and acetic acid anhydride for 30 min with silica as the milling auxiliary. To avoid using stainless steel in a corrosive environment and also potential contamination of the sample with iron by the action of acetic acid, all experiments were carried out in Teflon jars charged with a single 10 mm Teflon ball. The product was separated from silica by simply suspending the crude mixture in methanol, filtration and evaporation of the filtrate. To the best of our knowledge, this is the first example of paracetamol synthesis aided by milling mechanochemistry. NMR and IR analyses of the product **6** confirmed quantitative reaction and exclusive acetylation at the nitrogen atom. Each step (hydrogenation and acetylation) was also done on a gram scale producing **p-2c** (10 mmol, 1.09 g) and **6** (6.6 mmol, 0.99 g) in near quantitative isolated yields (99%). Paracetamol is known to crystallise in three polymorphic forms (form I, II and III) with distinctive physical properties important to pharmaceutical application [77–79]. Powder X-ray diffraction (PXRD) analysis showed that paracetamol synthesised mechanochemically by this route adopts the structure of form I (CSD refcode HXACAN01), which is the thermodynamically most stable polymorph (Figure S36, ESI).

In our previous studies, the solid state ball milling approach was established as the superior method for the synthesis of (thio)ureas by coupling amines with iso(thio)cyanates [80,81]. Particularly interesting feature of this method is the ability to quantitatively desymmetrise 1,2-phenylenediamine (**o-2b**) by reacting it with an equimolar amount of iso(thio)cyanate electrophile [82]. Sterically less demanding 1,4-phenylenediamine (**p-2b**) proved to be much more difficult substrate in this respect, resulting in a successful desymmetrisation reaction only with less reactive 4-methoxyphenyl isothiocyanate. For the same reason, milling 1,3-phenylenediamine (**m-2b**) with highly reactive phenyl isocyanate failed to selectively afford aminourea **2n-O** (21%) [83]. With the optimised mechanochemical CTH reaction conditions in hands, we now envisaged a three-step route to bis(urea) and hybrid urea-thiourea derivatives **7a,b** based on a 1,3-phenylene spacer group by integrating the solid state click-type amine-isocyanate coupling with the mechanochemical CTH of nitroarenes as the key "indirect" desymmetrization step (Scheme 2c). This approach produced the desymmetrized amino-urea **2n-O** in 88% yield (over two steps), which was then in the third step successfully transformed into bis(urea) **7a** (98%). Also, the introduction of a privileged 3,5-di(trifluoromethyl)phenyl structural motif in **7b** was accomplished in 93% yield, resulting in isolated yields for **7a,b** over three steps of 87% and 82%, respectively.

3. Materials and Methods

In a typical experiment, a mixture of nitroarene (1.0 mmol), ammonium formate (3.3 mmol, 208 mg, 1.1 equivalent based on the donor:substrate = 3:1 stoichiometry required for a quantitative reduction of the NO_2 to NH_2 functional group), 10 wt% palladium on carbon (21.0 mg, 2 mol%) and silica (175 mg) was loaded into a 10 mL stainless steel grinding jar along with one 12 mm diameter grinding ball. The mixture was ground in the presence of methanol as the grinding liquid ($\eta = 0.25 \mu L mg^{-1}$) for 90 min, unless otherwise stated (see Table 1). The crude product was scraped off the walls of the jar,

left in air overnight to allow excess ammonium formate to completely decompose and suspended in 10 mL of methanol. The suspension was filtered over a Büchner funnel and the filtrate was evaporated to afford amino derivatives. If necessary, the products were purified by column chromatography. Experimental details, spectroscopic and electron microscopy characterization data can be found in the Supplementary Materials.

4. Conclusions

We have successfully demonstrated that an efficient catalytic transfer hydrogenation of aromatic nitro compounds using readily available ammonium formate as hydrogen donor and palladium on carbon as the catalyst can be accomplished under solid-state mechanochemical milling conditions. The synthetic protocol, which is very simple and straightforward, tolerates a variety of functional groups, including amino, hydroxyl, carboxyl, carbamate, amide, imide, urea, acetyl, α,β -unsaturated carbonyl and fused heterocycles such as pyridine. The presence of halogen or *O*-benzyl substituents results in diminished yields, while polyaromatic substrates are not compatible. The mechanochemical approach has also been applied for the two-step synthesis of pharmaceutically important procainamide and paracetamol drugs, both on milligram and gram scale. We have also shown that the mechanochemical CTH can be coupled with the previously developed concept of click-mechanochemistry, to enable a multi-step synthesis of (thio)urea hybrid molecules as potential scaffolds in anion sensor and organocatalyst design.

Supplementary Materials: The following are available online at <http://www.mdpi.com/1420-3049/23/12/3163/s1>. General procedure for the mechanochemical reduction of nitroarenes, spectroscopic data for compounds **2a–x** and **4–7**, catalytic transfer hydrogenation of 3-nitrobenzotrile under aging conditions, SEM and EDS analysis of the commercial and milled Pd/C catalyst samples, MS and GC analysis of CTH of 4-chloro-2-nitroaniline (***o*-1p**) and 2-chloro-4-nitroaniline (***p*-1p**), ^1H and ^{13}C NMR spectra of selected compounds and PXRD analysis of mechanochemically-synthesized paracetamol (**6**). Figure S1: ^1H NMR spectrum of the crude reaction mixture after 6 h of milling under standard conditions (1.0 mmol scale, 1.1 eq HCOONH_4 , 2 mol% Pd/C) for the catalytic transfer hydrogenation of 1-nitronaphthalene (**1x**) to 1-aminonaphthalene (**2x**). Integration of the corresponding signals revealed the ratio **1x:2x** = 63:37, Figure S2: Aging experiments in vials of different volume. Each vial contained a mixture of 0.5 mmol of 3-nitrobenzotrile (**1a**), 1.65 mmol of HCOONH_4 (104 mg, 1.1 eq), 2 mol% of Pd/C catalyst (10.5 mg) and 87.5 mg of silica. This mixture was prepared by gentle manual grinding of **1a**, Pd/C and silica in a mortar, the resulting fine powder was then transferred to a vial, pre-ground ammonium formate was stirred in and quickly sealed. The final mixture was gently shaken in the vial for ca. 10 s and left undisturbed for 3 days, Figure S3: Representative ^1H NMR spectra of the mixture taken from the 10 mL vial immediately after opening and 24 h in air. The spectra were recorded in CDCl_3 . Notably, there is no significant change in the amount of 3-cyanoaniline (**2a**), confirming that upon exposure to air ("open system") the NO_2 -reduction stops and the primary reaction path becomes Pd-catalysed decomposition of HCOONH_4 , Figure S4: Representative IR spectra of the aging mixture from 10 mL vial immediately after opening, 4 h and 24 h in air. Ammonium formate decomposes in air revealing the absorption bands of **1a**, **2a** and silica after 24 h, Figure S5: Representative IR spectra of the aging mixture from 20 mL vial immediately after opening, 4 h and 24 h in air. Ammonium formate decomposes in air revealing the absorption bands of **1a** and silica after 24 h, Figure S6: SEM analysis of commercial Pd/C catalyst (10 wt%). (a–c) Typical morphology of carbon particles (ca. 10–100 μm) with palladium aggregates (shown in light grey to white) of different sizes (from ca. 100 nm to several μm) distributed on carbon surface (500 \times and 5000 \times). (d) A close-up view of one Pd aggregate (50,000 \times). Each aggregate is composed of many nanometre-sized Pd particles, Figure S7: SEM analysis of commercial Pd/C catalyst (10 wt%) milled for 60 min at 30 Hz using a single 12 mm (7.0 g) stainless steel ball. Morphology of the samples a–d (500 \times –10,000 \times) is characteristic for homogenization and pulverization of carbon particles during ball milling resulting in particle sizes ca. 0.5–5 μm , Figure S8: SEM-EDS analysis of commercial palladium on carbon (10 wt%). A distinctive feature of the catalyst as determined by SEM is the organization of palladium into aggregates (seen as small light particles) on the surface of larger carbon particles. (a) Analysis of the selected area on a large carbon particle shows traces of Pd, (b) point analysis on the same carbon particle identifies the palladium aggregate, (c) analysis of the selected area comprising both carbon particles and Pd aggregates, Figure S9: SEM-EDS analysis of (a) commercial Pd/C catalyst (10 wt%) milled for 60 min at 30 Hz using a single 12 mm (7.0 g) stainless steel ball shows a homogeneous distribution of Pd over the entire selected area, (b) Pd/C catalyst milled in the presence of silica under LAG conditions for 60 min, (c) a post-workup sample of the mixture containing Pd/C and silica after LAG reduction of **1a** to **2a** for 60 min. The intensity of Pd signal in EDS spectra under (b) and (c) is reduced because of dilution effect by added silica. All samples contain iron contamination (Fe^*) due to abrasion of stainless steel jar walls and the ball during milling, Figure S10: MS analysis of the methanol fraction after CTH of 4-chloro-2-nitroaniline (***o*-1p**) under standard conditions. 2,2'-Diaminoazobenzene ($M_r = 212$) and 2,2'-diamino-4-chloroazobenzene ($M_r = 246$) were identified as intermediates in the reaction mixture, which was consistent with the observed diminished yield (42%)

of 4-chloro-*o*-phenylenediamine (***o*-2p**) due to dehalogenation side reaction, Figure S11: GC analysis of the crude mixture after CTH of 4-chloro-2-nitroaniline (***o*-1p**). *o*-Phenylenediamine ($t_R = 4.18$ min) and *o*-nitroaniline ($t_R = 5.06$ min) are the by-products of dehalogenation side reaction. The reactant was consumed completely while the signal at $t_R = 5.22$ min corresponds to 4-chloro-*o*-phenylenediamine (***o*-2p**) product, Figure S12: GC analysis of the crude mixture after CTH of 2-chloro-4-nitroaniline (***p*-1p**). *p*-Phenylenediamine ($t_R = 4.41$ min) and *p*-nitroaniline ($t_R = 5.77$ min) are the by-products of dehalogenation side reaction. The reactant ($t_R = 6.06$ min) was not consumed completely while the signal at $t_R = 5.16$ min corresponds to 2-chloro-*p*-phenylenediamine (***p*-2p**) product, Figure S13: GC analysis of the crude mixture after CTH of 2-chloro-4-nitroaniline (***p*-1p**) with 2.2 eq of ammonium formate (6.6 mmol). *p*-Phenylenediamine ($t_R = 4.41$ min) and small amount of 2-chloro-*p*-phenylenediamine (***p*-2p**) were found as the only products, suggesting that dehalogenation became the primary reaction pathway, Figures S14–35: ^1H and ^{13}C NMR spectra of **2g–2r**, **2t–2w**, **5** and **7a–b**, Figure S36: PXRD analysis shows that mechanochemically-synthesized paracetamol (**6**) adopts the crystal structure of the thermodynamically most stable polymorph, form I.

Author Contributions: Conceptualization, V.Š. and T.P.; Methodology, V.Š.; Formal Analysis, V.Š., T.P. and D.M.; Investigation, V.Š., T.P. and D.M.; Resources, V.Š., T.P. and D.M.; Writing-Original Draft Preparation, V.Š.; Writing-Review & Editing, V.Š., T.P. and D.M.; Supervision, V.Š.; Project Administration, D.M.; Funding Acquisition, D.M.

Funding: This research was funded by the Croatian Science Foundation grant number 9310.

Acknowledgments: We thank Željka Petrović and Mira Ristić (RBI) for SEM analysis, Centre for NMR for recording NMR spectra (RBI) and Krunoslav Užarević (RBI) for PXRD measurements of paracetamol samples.

Conflicts of Interest: The authors declare no conflict of interest. The funding sponsors had no role in the design of the study; in the collection, analyses, or interpretation of data; in the writing of the manuscript and in the decision to publish the results.

References and Notes

1. Brieger, G.; Nestruck, T.J. Catalytic Transfer Hydrogenation. *Chem. Rev.* **1974**, *74*, 567–580. [[CrossRef](#)]
2. Wang, D.; Astruc, D. The Golden Age of Transfer Hydrogenation. *Chem. Rev.* **2015**, *115*, 6621–6686. [[CrossRef](#)] [[PubMed](#)]
3. Hagen, J. Heterogeneously Catalyzed Processes in Industry. In *Industrial Catalysis: A Practical Approach*, 2nd ed.; Hagen, J., Ed.; Wiley-VCH: Weinheim, Germany, 2006; pp. 261–293, ISBN 978-3-527-31144-6.
4. Ram, S.; Ehrekauf, R.E. Ammonium Formate in Organic Synthesis: A Versatile Agent in Catalytic Hydrogen Transfer Reductions. *Synthesis* **1988**, *1988*, 91–95. [[CrossRef](#)]
5. Zoran, A.; Sasson, Y. Catalytic transfer hydrogenation of unsaturated compounds by solid sodium formate in the presence of palladium on carbon. *J. Mol. Catal.* **1984**, *26*, 321–326. [[CrossRef](#)]
6. Paryzek, Z.; Koenig, H.; Tabaczka, B. Ammonium Formate/Palladium on Carbon: A Versatile System for Catalytic Hydrogen Transfer Reductions of Carbon-Carbon Double Bonds. *Synthesis* **2003**, 2023–2026. [[CrossRef](#)]
7. Dobrovolná, Z.; Červený, L. Ammonium formate decomposition using palladium catalyst. *Res. Chem. Intermed.* **2000**, *26*, 489–497. [[CrossRef](#)]
8. Banik, B.K.; Barakat, K.J.; Wagle, D.R.; Manhas, M.S.; Bose, A.K. Microwave-Assisted Rapid and Simplified Hydrogenation. *J. Org. Chem.* **1999**, *64*, 5746–5753. [[CrossRef](#)]
9. Vass, A.; Dudás, J.; Tóth, J.; Varma, R.S. Solvent-free reduction of aromatic nitro compounds with alumina-supported hydrazine under microwave irradiation. *Tetrahedron Lett.* **2001**, *42*, 5347–5349. [[CrossRef](#)]
10. Berthold, H.; Schotten, T.; Hönig, H. Transfer Hydrogenation in Ionic Liquids under Microwave Irradiation. *Synthesis* **2002**, 1607–1610. [[CrossRef](#)]
11. Do, J.-L.; Frišič, T. Mechanochemistry: A Force of Synthesis. *ACS Cent. Sci.* **2017**, *3*, 13–19. [[CrossRef](#)]
12. Howard, J.L.; Cao, Q.; Browne, D.L. Mechanochemistry as an emerging tool for molecular synthesis: What can it offer? *Chem. Sci.* **2018**, *9*, 3080–3094. [[CrossRef](#)] [[PubMed](#)]
13. Xu, C.; De, S.; Balu, A.M.; Ojeda, M.; Luque, R. Mechanochemical synthesis of advanced nanomaterials for catalytic applications. *Chem. Commun.* **2015**, *51*, 6698–6713. [[CrossRef](#)]
14. Gečiauskaite, A.A.; García, F. Main group mechanochemistry. *Beilstein J. Org. Chem.* **2017**, *13*, 2068–2077. [[CrossRef](#)] [[PubMed](#)]

15. André, V.; Quaresma, S.; da Silva, J.L.F.; Duarte, M.T. Exploring mechanochemistry to turn organic bio-relevant molecules into metal-organic frameworks: A short review. *Beilstein J. Org. Chem.* **2017**, *13*, 2416–2427. [[CrossRef](#)] [[PubMed](#)]
16. Wixtrom, A.; Buhler, J.; Abdel-Fattah, T. Mechanochemical Synthesis of Two Polymorphs of the Tetrathiafulvalene–Chloranil Charge Transfer Salt: An Experiment for Organic Chemistry. *J. Chem. Educ.* **2014**, *91*, 1232–1235. [[CrossRef](#)]
17. Crawford, D.E.; Miskimmin, C.K.G.; Albadarin, A.B.; Walker, G.; James, S.L. Organic synthesis by Twin Screw Extrusion (TSE): Continuous, scalable and solvent-free. *Green Chem.* **2017**, *19*, 1507–1518. [[CrossRef](#)]
18. Crawford, D.E.; Wright, L.A.; James, S.L.; Abbott, A.P. Efficient continuous synthesis of high purity deep eutectic solvents by twin screw extrusion. *Chem. Commun.* **2016**, *52*, 4215–4218. [[CrossRef](#)]
19. Crawford, D.; Casaban, J.; Haydon, R.; Giri, N.; McNally, T.; James, S.L. Synthesis by extrusion: Continuous, large-scale preparation of MOFs using little or no solvent. *Chem. Sci.* **2015**, *6*, 1645–1649. [[CrossRef](#)]
20. Michalchuk, A.A.L.; Hope, K.S.; Kennedy, S.R.; Blanco, M.V.; Boldyreva, E.V.; Pulham, C.R. Ball-free mechanochemistry: In situ real-time monitoring of pharmaceutical co-crystal formation by resonant acoustic mixing. *Chem. Commun.* **2018**, *54*, 4033–4036. [[CrossRef](#)]
21. Martina, K.; Rotolo, L.; Porcheddu, A.; Delogu, F.; Bysouth, S.R.; Cravotto, G.; Colacino, E. High throughput mechanochemistry: Application to parallel synthesis of benzoxazines. *Chem. Commun.* **2018**, *54*, 551–554. [[CrossRef](#)]
22. Štrukil, V.; Sajko, I. Mechanochemically-assisted solid-state photocatalysis (MASSPC). *Chem. Commun.* **2017**, *53*, 9101–9104. [[CrossRef](#)] [[PubMed](#)]
23. Wang, G.-W. Mechanochemical organic synthesis. *Chem. Soc. Rev.* **2013**, *42*, 7668–7700. [[CrossRef](#)]
24. Štrukil, V. Mechanochemical Organic Synthesis: The Art of Making Chemistry Green. *Synlett* **2018**, *29*, 1281–1288. [[CrossRef](#)]
25. Tan, D.; Friščić, T. Mechanochemistry for Organic Chemists: An Update. *Eur. J. Org. Chem.* **2018**, 18–33. [[CrossRef](#)]
26. Colacino, E.; Porcheddu, A.; Halasz, I.; Charnay, C.; Delogu, F.; Guerra, R.; Fullenwarth, J. Mechanochemistry for “no solvent, no base” preparation of hydantoin-based active pharmaceutical ingredients: Nitrofurantoin and dantrolene. *Green Chem.* **2018**, *20*, 2973–2977. [[CrossRef](#)]
27. Andersen, J.; Mack, J. Mechanochemistry and organic synthesis: From mystical to practical. *Green Chem.* **2018**, *20*, 1435–1443. [[CrossRef](#)]
28. Chauhan, P.; Chimni, S.S. Mechanochemistry assisted asymmetric organocatalysis: A sustainable approach. *Beilstein J. Org. Chem.* **2012**, *8*, 2132–2141. [[CrossRef](#)]
29. Rodríguez, B.; Rantanen, T.; Bolm, C. Solvent-Free Asymmetric Organocatalysis in a Ball Mill. *Angew. Chem. Int. Ed.* **2006**, *45*, 6924–6926. [[CrossRef](#)]
30. Rantanen, T.; Schiffrers, I.; Bolm, C. Solvent-Free Asymmetric Anhydride Opening in a Ball Mill. *Org. Process Res. Dev.* **2007**, *11*, 592–597. [[CrossRef](#)]
31. Hernández, J.G.; Friščić, T. Metal-catalyzed organic reactions using mechanochemistry. *Tetrahedron Lett.* **2015**, *56*, 4253–4265. [[CrossRef](#)]
32. Hernández, J.G. C–H Bond Functionalization by Mechanochemistry. *Chem. Eur. J.* **2017**, *23*, 17157–17165. [[CrossRef](#)] [[PubMed](#)]
33. Zhao, S.; Li, Y.; Liu, C.; Zhao, Y. Recent advances in mechanochemical C–H functionalization reactions. *Tetrahedron Lett.* **2018**, *59*, 317–324. [[CrossRef](#)]
34. Leonardi, M.; Villacampa, M.; Menéndez, J.C. Multicomponent mechanochemical synthesis. *Chem. Sci.* **2018**, *9*, 2042–2064. [[CrossRef](#)] [[PubMed](#)]
35. Delogu, F.; Mulas, G.; Garroni, S. Hydrogenation of carbon monoxide under mechanical activation conditions. *Appl. Catal. A Gen.* **2009**, *366*, 201–205. [[CrossRef](#)]
36. Mack, J.; Fulmer, D.; Stofel, S.; Santos, N. The first solvent-free method for the reduction of esters. *Green Chem.* **2007**, *9*, 1041–1043. [[CrossRef](#)]
37. Kaupp, G. Organic Solid-State Reactions with 100% Yield. *Top. Curr. Chem.* **2005**, *254*, 95–183, (pp. 117, unpublished results). [[CrossRef](#)]
38. Birke, V.; Mattik, J.; Runne, D. Mechanochemical reductive dehalogenation of hazardous polyhalogenated contaminants. *J. Mat. Sci.* **2004**, *39*, 5111–5116. [[CrossRef](#)]

39. Lu, S.; Huang, J.; Peng, Z.; Li, X.; Yan, J. Ball milling 2,4,6-trichlorophenol with calcium oxide: Dechlorination experiment and mechanism considerations. *Chem. Eng. J.* **2012**, *195*, 62–68. [[CrossRef](#)]
40. Loisel, S.; Branca, M.; Mulas, G.; Cocco, G. Selective Mechanochemical Dehalogenation of Chlorobenzenes over Calcium Hydride. *Environ. Sci. Technol.* **1996**, *31*, 261–265. [[CrossRef](#)]
41. Pri-Bar, I.; James, B.R. Mechanochemical, solvent free, palladium-catalyzed hydrodechlorination of chloroaromatic hydrocarbons. *J. Mol. Catal. A Chem.* **2007**, *264*, 135–139. [[CrossRef](#)]
42. Sawama, Y.; Kawajiri, T.; Niikawa, M.; Goto, R.; Yabe, Y.; Takahashi, T.; Marumoto, T.; Itoh, M.; Kimura, Y.; Monguchi, Y.; et al. Stainless-Steel Ball-Milling Method for Hydro-/Deutero-genation using H₂O/D₂O as a Hydrogen/Deuterium Source. *ChemSusChem* **2015**, *8*, 3773–3776. [[CrossRef](#)] [[PubMed](#)]
43. Sawama, Y.; Niikawa, M.; Yabe, Y.; Goto, R.; Kawajiri, T.; Marumoto, T.; Takahashi, T.; Itoh, M.; Kimura, Y.; Sasai, Y.; et al. Stainless-Steel-Mediated Quantitative Hydrogen Generation from Water under Ball Milling Conditions. *ACS Sustain. Chem. Eng.* **2015**, *3*, 683–689. [[CrossRef](#)]
44. Sawama, Y.; Yasukawa, N.; Ban, K.; Goto, R.; Niikawa, M.; Monguchi, Y.; Itoh, M.; Sajiki, H. Stainless Steel-Mediated Hydrogen Generation from Alkanes and Diethyl Ether and Its Application for Arene Reduction. *Org. Lett.* **2018**, *20*, 2892–2896. [[CrossRef](#)] [[PubMed](#)]
45. Manuel, S.; Léger, B.; Addad, A.; Monflier, E.; Hapiot, F. Cyclodextrins as effective additives in AuNP-catalyzed reduction of nitrobenzene derivatives in a ball-mill. *Green Chem.* **2016**, *18*, 5500–5509. [[CrossRef](#)]
46. Li, A.Y.; Segalla, A.; Li, C.-J.; Moores, A. Mechanochemical Metal-Free Transfer Hydrogenation of Carbonyls Using Polymethylhydrosiloxane as the Hydrogen Source. *ACS Sustain. Chem. Eng.* **2017**, *5*, 11752–11760. [[CrossRef](#)]
47. Kadam, H.K.; Tilve, S.G. Advancement in methodologies for reduction of nitroarenes. *RSC Adv.* **2015**, *5*, 83391–83407. [[CrossRef](#)]
48. Zhao, Z.; Yang, H.; Li, Y.; Guo, X. Cobalt-modified molybdenum carbide as an efficient catalyst for chemoselective reduction of aromatic nitro compounds. *Green Chem.* **2014**, *16*, 1274–1281. [[CrossRef](#)]
49. Yang, X.-J.; Chen, B.; Zheng, L.-Q.; Wu, L.-Z.; Tung, C.-H. Highly efficient and selective photocatalytic hydrogenation of functionalized nitrobenzenes. *Green Chem.* **2014**, *16*, 1082–1086. [[CrossRef](#)]
50. Wang, L.; Li, P.; Wu, Z.; Yan, J.; Wang, M.; Ding, Y. Reduction of Nitroarenes to Aromatic Amines with Nanosized Activated Metallic Iron Powder in Water. *Synthesis* **2003**, 2001–2004. [[CrossRef](#)]
51. Wienhöfer, G.; Baseda-Krüger, M.; Ziebart, C.; Westerhaus, F.A.; Baumann, W.; Jackstell, R.; Junge, K.; Beller, M. Hydrogenation of nitroarenes using defined iron–phosphine catalysts. *Chem. Commun.* **2013**, *49*, 9089–9091. [[CrossRef](#)]
52. Vaidya, M.J.; Kulkarni, S.M.; Chaudhari, R.V. Synthesis of *p*-Aminophenol by Catalytic Hydrogenation of *p*-Nitrophenol. *Org. Process Res. Dev.* **2003**, *7*, 202–208. [[CrossRef](#)]
53. Baron, M.; Méta, E.; Lemaire, M.; Popowycz, F. Reduction of aromatic and aliphatic nitro groups to anilines and amines with hypophosphites associated with Pd/C. *Green Chem.* **2013**, *15*, 1006–1015. [[CrossRef](#)]
54. Orlandi, M.; Brenna, D.; Harms, R.; Jost, S.; Benaglia, M. Recent Developments in the Reduction of Aromatic and Aliphatic Nitro Compounds to Amines. *Org. Process Res. Dev.* **2018**, *22*, 430–445. [[CrossRef](#)]
55. Ram, S.; Ehrekauf, R.E. A general procedure for mild and rapid reduction of aliphatic and aromatic nitro compounds using ammonium formate as a catalytic hydrogen transfer agent. *Tetrahedron Lett.* **1984**, *25*, 3415–3418. [[CrossRef](#)]
56. Ram, S.; Ehrekauf, R.E. A Facile Synthesis of α -Amino Esters via Reduction of α -Nitro Esters Using Ammonium Formate as a Catalytic Hydrogen Transfer Agent. *Synthesis* **1986**, 133–135. [[CrossRef](#)]
57. HPLC analysis showed that the CTH of 3-nitrobenzotrionitrile (**1a**) (1.0 mmol) in methanol solution (10 mL) with 3 eq of ammonium formate (9.9 mmol) reached quantitative yield in 30 minutes.
58. Đud, M.; Magdysyuk, O.V.; Margetić, D.; Štrukil, V. Synthesis of monosubstituted thioureas by vapour digestion and mechanochemical amination of thiocarbamoyl benzotriazoles. *Green Chem.* **2016**, *18*, 2666–2674. [[CrossRef](#)]
59. The reaction mass loss upon opening the jars indicated ca. 60% conversion after 1 hour and quantitative decomposition after 2 hours in air.
60. Rajagopal, S.; Anwer, M.K.; Spatola, A.F. Catalytic transfer hydrogenation and hydrogenolysis by formic acid and its salts. In *Peptides Design, Synthesis, and Biological Activity*, 1st ed.; Basava, C., Anantharamaiah, G.M., Eds.; Birkhäuser: Boston, MA, USA, 1994; Chapter 2, pp. 11–26, ISBN 978-1-4615-8178-9.

61. Byun, E.; Hong, B.; De Castro, K.A.; Lim, M.; Rhee, H. One-Pot Reductive Mono-*N*-alkylation of Aniline and Nitroarene Derivatives Using Aldehydes. *J. Org. Chem.* **2007**, *72*, 9815–9817. [[CrossRef](#)]
62. Tuteja, J.; Nishimura, S.; Ebitani, K. Base-free chemoselective transfer hydrogenation of nitroarenes to anilines with formic acid as hydrogen source by a reusable heterogeneous Pd/ ZrP catalyst. *RSC Adv.* **2014**, *4*, 38241–38249. [[CrossRef](#)]
63. The reaction volume change is defined as the difference between the sums of molar volumes of products and reactants, $\Delta_r V = \sum V_m(\text{products}) - \sum V_m(\text{reactants})$. For solids, the difference in molar volumes is typically small and can be neglected. With this assumption, the CTH will generate 2 moles of gaseous products per 1 mole of the formate salt, while the complete decomposition of HCOONH₄ will result in 3 moles of gases per 1 mole of the salt. Therefore, $\Delta_r V_1$ (decomposition) > $\Delta_r V_2$ (CTH).
64. Maegawa, T.; Fujiwara, Y.; Ikawa, T.; Hisashi, H.; Monguchi, Y.; Sajiki, H. Novel deprotection method of Fmoc group under neutral hydrogenation conditions. *Amino Acids* **2009**, *36*, 493–499. [[CrossRef](#)]
65. Albers, P.; Pietsch, J.; Parker, S.F. Poisoning and deactivation of palladium catalysts. *J. Mol. Catal. A Chem.* **2001**, *173*, 275–286. [[CrossRef](#)]
66. Choudhary, V.R.; Sane, M.G. Poisoning of Pd-carbon catalysts by sulphur, chloro and heavy metal compounds in liquid phase hydrogenation of *o*-nitrophenol to *O*-aminophenol. *J. Chem. Technol. Biotechnol.* **1998**, *73*, 336–340. [[CrossRef](#)]
67. Kulla, H.; Fischer, F.; Benemann, S.; Rademann, K.; Emmerling, F. The effect of the ball to reactant ratio on mechanochemical reaction times studied by in situ PXRD. *Cryst. Eng. Comm.* **2017**, *19*, 3902–3907. [[CrossRef](#)]
68. As suggested by preliminary DFT calculations (B97D/6-31G(d) method), the reason behind the observed poor reactivity of these substrates could be a strong π -interaction of polyaromatic molecules with graphite-like structure of activated carbon, where the formation of 1:1 or 1:2 sandwich complexes might interfere with the reduction of the nitro group. The stability of such 1:1 and 1:2 complexes increases with the number of condensed aromatic rings in nitroarene substrates. For instance, the relative energies of 1:1 complexes of nitrobenzene, 1-amino and 2-aminonaphthalene, 1-amino and 2-aminoanthracene and 1-aminopyrene, with coronene as a graphite-like model structure are –13.6, –18.3, –16.1, –21.0, –21.7 and –24.1 kcal mol^{–1}, respectively. By employing the M062X/6-31G(d) method, these values were found to follow the same trend, but with less pronounced relative energy difference: –12.1, –15.7, –16.5, –17.9, –18.9 and –19.3 kcal mol^{–1}.
69. Shannon, S.K.; Peacock, M.J.; Kates, S.A.; Barany, G. Solid-Phase Synthesis of Lidocaine and Procainamide Analogues Using Backbone Amide Linker (BAL) Anchoring. *J. Comb. Chem.* **2003**, *5*, 860–868. [[CrossRef](#)] [[PubMed](#)]
70. Tan, D.; Loots, L.; Friščić, T. Towards medicinal mechanochemistry: Evolution of milling from pharmaceutical solid form screening to the synthesis of active pharmaceutical ingredients (APIs). *Chem. Commun.* **2016**, *52*, 7760–7781. [[CrossRef](#)]
71. Métro, T.-X.; Bonnamour, J.; Reidon, T.; Sarpoulet, J.; Martinez, J.; Lamaty, F. Mechanochemical synthesis of amides in the total absence of organic solvent from reaction to product recovery. *Chem. Commun.* **2012**, *48*, 11781–11783. [[CrossRef](#)]
72. Bonnamour, J.; Métro, T.-X.; Martinez, J.; Lamaty, F. Environmentally benign peptide synthesis using liquid-assisted ball-milling: Application to the synthesis of Leu-enkephalin. *Green Chem.* **2013**, *15*, 1116–1120. [[CrossRef](#)]
73. Estévez, V.; Villacampa, M.; Menéndez, J.C. Concise synthesis of atorvastatin lactone under high-speed vibration milling conditions. *Org. Chem. Front.* **2014**, *1*, 458–463. [[CrossRef](#)]
74. Tan, D.; Štrukil, V.; Mottillo, C.; Friščić, T. Mechanochemical synthesis of pharmaceutically relevant sulfonyl-(thio)ureas. *Chem. Commun.* **2014**, *50*, 5248–5250. [[CrossRef](#)]
75. Rajput, L.; Banerjee, R. Mechanochemical Synthesis of Amide Functionalized Porous Organic Polymers. *Cryst. Growth Des.* **2014**, *14*, 2729–2732. [[CrossRef](#)]
76. Yang, Y.; Bu, F.; Liu, J.; Shakir, I.; Xu, Y. Mechanochemical synthesis of two-dimensional aromatic polyamides. *Chem. Commun.* **2017**, *53*, 7481–7484. [[CrossRef](#)]
77. Perlovich, G.L.; Volkova, T.V.; Bauer-Brandl, A. Polymorphism of paracetamol. *J. Therm. Anal. Calorim.* **2007**, *89*, 767–774. [[CrossRef](#)]
78. Di Martino, P.; Conflant, P.; Drache, M.; Huvenne, J.-P.; Guyot-Hermann, A.-M. Preparation and physical characterization of forms II and III of paracetamol. *J. Therm. Anal.* **1997**, *48*, 447–458. [[CrossRef](#)]

79. Telford, R.; Seaton, C.C.; Clout, A.; Buanz, A.; Gaisford, S.; Williams, G.R.; Prior, T.J.; Okoye, C.H.; Munshi, T.; Scowen, I.J. Stabilisation of metastable polymorphs: The case of paracetamol form III. *Chem. Commun.* **2016**, *52*, 12028–12031. [[CrossRef](#)] [[PubMed](#)]
80. Štrukil, V.; Igrc, M.D.; Eckert-Maksić, M.; Friščić, T. Click Mechanochemistry: Quantitative Synthesis of “Ready to Use” Chiral Organocatalysts by Efficient Two-Fold Thiourea Coupling to Vicinal Diamines. *Chem. Eur. J.* **2012**, *18*, 8464–8473. [[CrossRef](#)] [[PubMed](#)]
81. Štrukil, V.; Igrc, M.D.; Fábíán, L.; Eckert-Maksić, M.; Childs, S.L.; Reid, D.G.; Duer, M.J.; Halasz, I.; Mottillo, C.; Friščić, T. A model for a solvent-free synthetic organic research laboratory: Click-mechanosynthesis and structural characterization of thioureas without bulk solvents. *Green Chem.* **2012**, *14*, 2462–2473. [[CrossRef](#)]
82. Štrukil, V.; Margetić, D.; Igrc, M.D.; Eckert-Maksić, M.; Friščić, T. Desymmetrisation of aromatic diamines and synthesis of non-symmetrical thiourea derivatives by click-mechanochemistry. *Chem. Commun.* **2012**, *48*, 9705–9707. [[CrossRef](#)] [[PubMed](#)]
83. Neat grinding of equimolar amounts of *m*-phenylenediamine (***m*-2b**) and phenyl isocyanate for 30 minutes using one 12 mm stainless steel ball led to a mixture of unreacted diamine (21%), isocyanate (4%), amino-urea **2n-O** (21%) and bis(urea) **7a** (54%), based on ¹H NMR analysis. For comparison, sterically more hindered *o*-phenylenediamine (***o*-2b**) afforded the respective amino-urea in 78% under the same conditions.

Sample Availability: Not available.



© 2018 by the authors. Licensee MDPI, Basel, Switzerland. This article is an open access article distributed under the terms and conditions of the Creative Commons Attribution (CC BY) license (<http://creativecommons.org/licenses/by/4.0/>).